Symmetry-induced nonequilibrium distributions of bright and dark exciton states in single carbon nanotubes

Ryusuke Matsunaga,[1] Yuhei Miyauchi,[1] Kazunari Matsuda,[1,*] and Yoshihiko Kanemitsu[1,2,†]
[1]*Institute for Chemical Research, Kyoto University, Uji, Kyoto 611-0011, Japan*
[2]*Photonics and Electronics Science and Engineering Center, Kyoto University, Kyoto 615-8510, Japan*
(Received 10 May 2009; revised manuscript received 28 July 2009; published 30 September 2009)

We investigated the magnetic and temperature dependence of the bright and dark exciton luminescence spectra in single carbon nanotubes. We found that the phonon-induced exciton scattering rate from the bright to the dark state is only one order of magnitude larger than the dark exciton recombination rate below 10 K at zero magnetic field. Our results indicate that excitons are nonequilibriumly distributed between the bright and dark states due to the different parities of the wave functions and that Aharonov-Bohm flux enhances the phonon-induced exciton scattering between these two states. Our nonequilibrium exciton distribution model can also explain the nonzero photoluminescence intensity at very low temperatures.

DOI: 10.1103/PhysRevB.80.115436 PACS number(s): 78.67.Ch, 63.20.kk, 71.35.Ji, 78.55.Kz

I. INTRODUCTION

The optical properties of semiconducting carbon nanotubes, originating from one-dimensional stable excitons, have been under intense investigation both for their fundamental physics interest and their potential applicability in optical devices.[1–3] Theoretical studies have predicted that the degenerated two valleys create multiple exciton states.[4–8] Only the odd-parity exciton, with spin singlet and zero angular momentum, called the *bright* exciton, can recombine radiatively; the other exciton states are all dipole-forbidden (*dark*). Thus, the experimental observation of dark excitons is very important in understanding the excitonic nature of carbon nanotubes. The Aharonov-Bohm (AB) effect induced by the magnetic field threading the tube axis[9] makes even-parity singlet dark exciton partially dipole allowed,[8] which has led to photoluminescence (PL) and absorption experiments under high magnetic fields.[10–16] Recently, direct evidence for the singlet dark exciton state a few meV below the bright exciton state has been reported by magneto-PL spectroscopy for single carbon nanotubes.[17,18]

The exciton populations of the bright and dark states have usually been described by assuming a Boltzmann distribution.[6,7,12,13,18] Relaxation scheme for reaching a Boltzmann distribution is the same as Kasha's rule in molecular systems, where the relaxation rate from the higher states to the lowest singlet state is much larger than the radiative and nonradiative relaxation rates of the lowest singlet state.[19] However, the characteristics of the singlet exciton states arising from Coulomb interactions between the degenerated two valleys in carbon nanotubes are quite different from those in molecules and nanocrystal quantum dots.[20,21] Although many time-resolved measurements for carbon nanotubes have been reported,[22–27] exciton dynamics and distributions between the exciton fine structures remain a matter of intense debate. Thus, it is necessary to experimentally elucidate the exciton distribution between the bright and dark states by means of direct information on the dark exciton state for understanding the optical properties of carbon nanotubes.

In this paper, we studied the exciton distribution between the bright and dark states through the magnetic and temperature dependences of the PL spectra of single carbon nanotubes. Our results show that excitons are nonequilibriumly distributed between the bright and dark states due to the different parities of the wave functions, and that AB flux enhances the phonon-induced exciton scattering between the two states. We also found that the temperature dependence of the PL intensity can be explained by our nonequilibrium exciton distribution model.

II. EXPERIMENTAL METHOD

The samples used in the single nanotube spectroscopy were single-walled carbon nanotubes synthesized on Si substrates using an alcohol catalytic chemical vapor deposition method.[28] Each observed nanotube was suspended over patterned grooves, typically of 5 μm width and depth, which were fabricated on Si substrates using an electron-beam lithography technique. Spatially isolated single carbon nanotubes without surfactants provided us with inherent information on their excitonic properties.[17,29–32] In addition, we prepared carbon nanotube samples dispersed in poly[9,9-dioctylfluorenyl-2,7-diyl] (PFO) to investigate the ensemble-averaged PL intensity. These carbon nanotubes were isolated by dispersion in a toluene solution with 0.07 wt. % PFO, 60 min of moderate bath sonication, 15 min of vigorous sonication with a tip-type sonicator, and centrifugation at an acceleration of 13 000 g for 5 min.[33] The PFO-dispersed carbon nanotubes were deposited on quartz substrates.

The magneto-PL spectroscopy of single carbon nanotubes was carried out in the Voigt geometry using a home-built variable-temperature confocal microscope (NA 0.5) and a He-Ne laser (1.96 eV) with the excitation laser light propagating perpendicular to the magnetic field.[17] The samples were mounted in a cryostat under a superconducting magnet with fields up to 7 T. The PL signals from single carbon nanotubes were detected by a 30 cm spectrometer equipped with a liquid-nitrogen-cooled InGaAs photodiode array. The spectral resolution of the system was below 1.0 meV.

III. RESULTS AND DISCUSSION

Figures 1(a) and 1(b) show magneto-PL spectra at 9 K for single carbon nanotubes [assigned chiral index: (11,3) and

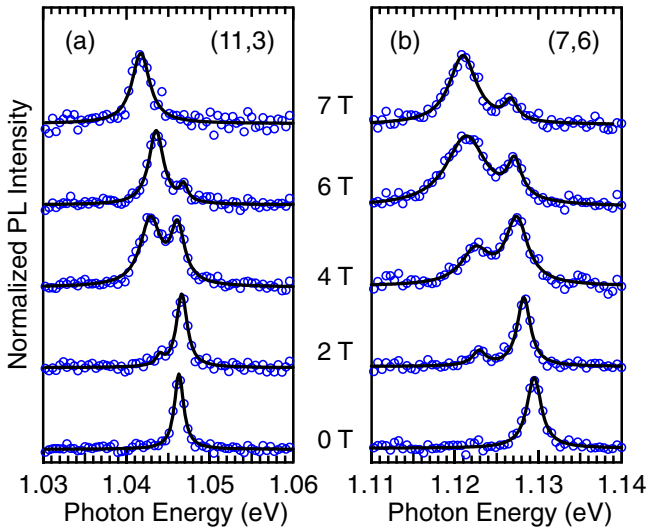

FIG. 1. (Color online) (a) and (b) Normalized magneto-PL spectra in the Voigt geometry at 9 K for single (11,3) and (7,6) nanotubes, respectively. Angles between the tube axes and the magnetic field were estimated ~0° and 5° by polarized absorption properties. (Ref. 17)

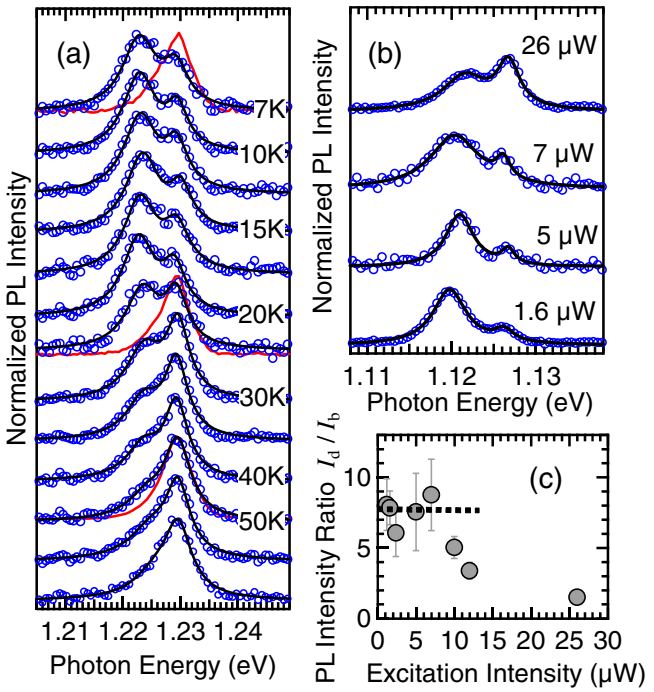

FIG. 2. (Color online) (a) Temperature dependence of magneto-PL spectra at 7 T for a single (7,5) nanotube. The red lines show PL spectra at 0 T. (b) Magneto-PL spectra at 7 T for a (7,6) carbon nanotube under various excitation laser powers. (c) Laser-power dependence of the PL intensity ratio of the dark to the bright excitons in the (b).

(7,6), respectively]. While a single sharp PL originating from the bright exciton state is observed at zero magnetic field, another PL peak appears a few meV below the bright exciton peak under the magnetic fields parallel to the tube axis. These PL spectra are fit by double-Lorentzian functions in Figs. 1(a) and 1(b). With increasing magnetic field, the lower-energy peak grows and redshifts, which can be understood in terms of dark exciton brightening due to the magnetic flux threading the tube axis (AB flux).[8,11] From the splitting induced by the AB flux, we determined that the splitting energies between the bright and dark exciton states at 0 T were about 2.6 and 4.5 meV in Figs. 1(a) and 1(b), respectively.[17]

A. Temperature dependence of exciton distribution

Figure 2(a) shows the temperature dependence of the magneto-PL spectra for a (7,5) nanotube in a 7 T field. The PL peak from the dark exciton state is more clearly observed at lower temperatures. This result can be explained by the concentrating of the population in the lower dark exciton state with decreasing temperature, as the PL intensity can be represented as the product of the oscillator strength and the population of excitons. We also checked the magneto-PL spectra for a single carbon nanotube at various excitation laser powers in Fig. 2(b). If nanotubes are heated by the excitation laser, the PL intensity ratio of the dark to the bright excitons rapidly decreases with increasing the laser power. In our weak excitation conditions below a few microwatts, however, the PL intensity ratio was independent of the laser power as shown in Fig. 2(c). We therefore concluded that heating of the nanotubes due to excitation laser could be neglected in this work.

We investigated the exciton population from the PL intensity ratio of the dark to the bright excitons, I_d/I_b. Figure 3(a) shows the temperature dependence of I_d/I_b at a magnetic field of 7 T for the (7,5) carbon nanotube shown in Fig. 2(a). While I_d/I_b (solid circles) in Fig. 3(a) increases with decreasing temperature, it clearly saturates below 20 K. In a Boltzmann exciton distribution, I_d/I_b should diversely increase toward low temperatures [the thick solid black line in Fig. 3(a)] because the exciton population fully concentrates on the lower dark state. However, the experimental data do not diverge as rapidly as expected for a Boltzmann distribution.

We consider the transition rates between the bright and dark exciton states at 7 T to understand the experimental results. Inset of Fig. 3 shows a schematic of a three-level model consisting of the bright and dark exciton states with a splitting energy Δ and a ground state.[26,27] The lifetimes of the bright and dark excitons are denoted as $1/\Gamma_b$ and $1/\Gamma_d$, respectively. Γ_b includes both the radiative decay rate Γ_R and the nonradiative decay rate Γ_{NR}. Assuming the one phonon absorption and emission process, we can represent the downward and upward scattering rate between the bright and dark exciton states as $\gamma_\downarrow = \gamma_0(n+1)$ and $\gamma_\uparrow = \gamma_0 n$, respectively, where $n = 1/[\exp(\Delta/k_B T) - 1]$ is the phonon occupation number and γ_0 is the temperature-independent scattering rate. The rate equation for the dark exciton population can be expressed as

$$\frac{dN_d}{dt} = \gamma_\downarrow N_b - (\gamma_\uparrow + \Gamma_d) N_d, \tag{1}$$

where N_b and N_d are the populations of the bright and dark exciton states, respectively. In the steady state ($dN_d/dt = 0$),

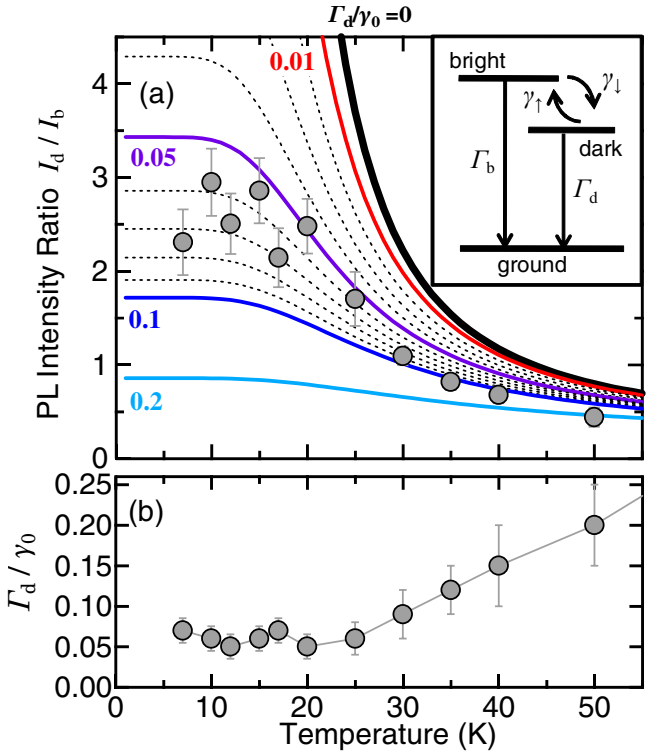

FIG. 3. (Color online) (a) Temperature dependence of the PL intensity ratio of the dark to the bright excitons at 7 T for the (7,5) nanotube. The circles show experimental results and the lines indicate the calculated results for each Γ_d/γ_0. (b) Temperature dependence of Γ_d/γ_0 evaluated from (a). Inset: Schematic of a three-level model, with the bright and dark exciton states and a ground state.

the population ratio of the dark to the bright exciton state is

$$\frac{N_d}{N_b} = \frac{\exp(\Delta/k_B T)}{1 + \frac{\Gamma_d}{\gamma_0}[\exp(\Delta/k_B T) - 1]}. \quad (2)$$

This equation indicates that N_d/N_b depends on the parameter Γ_d/γ_0, the ratio of the dark exciton lifetime to the thermalization time between the two exciton states. If the phonon-induced exciton scattering rate γ_0 is large enough at a given temperature, the term $(\Gamma_d/\gamma_0)[\exp(\Delta/k_B T)-1]$ in Eq. (2) can be neglected and N_d/N_b simplifies to $\exp(\Delta/k_B T)$, a Boltzmann distribution. The thick solid black line in Fig. 3(a) shows the calculated I_d/I_b, assuming the Boltzmann distribution $(\Gamma_d/\gamma_0 \to 0)$ between the bright and dark exciton states. Here, we calculated the relative oscillator strength of the dark to the bright excitons in the simplified model[13] as

$$\frac{f_d}{f_b} = \frac{1 - \frac{\Delta_{bd}}{\Delta}}{1 + \frac{\Delta_{bd}}{\Delta}}, \quad (3)$$

where Δ_{bd} is the zero-field splitting energy between the bright and dark exciton states.[17] The other lines in Fig. 3(a) correspond to the calculated results for each value of Γ_d/γ_0. In this temperature region I_d/I_b is strongly dependent on Γ_d/γ_0. Below 20 K, the calculated line for $\Gamma_d/\gamma_0 = 0.06 \pm 0.02$ reproduces the experimental data well.

We determined the values of Γ_d/γ_0 for each temperature from the experimental data in Fig. 3(a), and plotted them as a function of temperature in Fig. 3(b). Since γ_0 is temperature independent, we can obtain the temperature dependence of the dark exciton decay rate Γ_d, which is dominated by the nonradiative process. The Γ_d is almost constant below about 20 K and becomes large with increasing temperature. At room temperature, up to 7 T, we could hardly observe the dark exciton PL peak even though the term $\exp(\Delta/k_B T)-1$ is small. Therefore we concluded that Γ_d/γ_0 is at least larger than 1 at room temperature at 7 T. A consistent result has been recently reported by using time-resolved spectroscopy for single carbon nanotubes.[27]

Our result suggests that the phonon-induced exciton scattering between the bright and dark states does not occur rapidly as compared to the dark exciton lifetime. This means that the excitons are not fully thermalized between the two states. Theory predicts that phonons cannot scatter excitons between these two states for ideal carbon nanotubes because the bright and dark excitons have odd and even parities, respectively, and the phonon cannot break the symmetry.[6] Therefore, the slow phonon-induced exciton scattering between the bright and dark states leading to the non-Boltzmann distribution can be explained by the different parities of the two exciton states.

B. Magnetic-field dependence of exciton distribution

Figures 4(a)–4(c) show PL intensity ratio I_d/I_b as a function of magnetic field for different nanotubes at 7–9 K. Dark exciton PL peak becomes dominant with increasing magnetic field. The I_d/I_b curves calculated from the product of Eqs. (2) and (3), with different Γ_d/γ_0 are also shown in Figs. 4(a)–4(c). The experimental data are lower than the thick solid black line, which assumes a Boltzmann exciton distribution, at lower magnetic fields and become close to the calculated curves with smaller Γ_d/γ_0 for increasing magnetic field.

In Fig. 5, we plotted Γ_d/γ_0 for each nanotube at 7–9 K as a function of the AB flux per the magnetic quantum $\phi_0 = ch/e$, where the AB flux is calculated by $\phi = (\pi d^2/4)B \cos\alpha$ using the tube diameter d and the angle α between the tube axis and the magnetic field B.[17] With increasing the AB flux ϕ, the values of Γ_d/γ_0 rapidly decrease in Fig. 5. If we assume that Γ_d determined by the nonradiative decay is almost independent of the magnetic field, the change in Γ_d/γ_0 arises from γ_0. The phonon-induced exciton scattering rate γ_0, determined by the transition matrix element between the bright and dark states, should become large with increasing magnetic field because the AB effect causes symmetry breaking;[8] the parities of the wave functions for the bright and dark excitons gradually changes. Therefore, phonons can scatter excitons between the bright and dark states and the exciton distribution comes closer to a Boltzmann distribution at high magnetic fields. Figure 5 suggests that the AB flux causes the increase in γ_0 by the symmetry breaking.

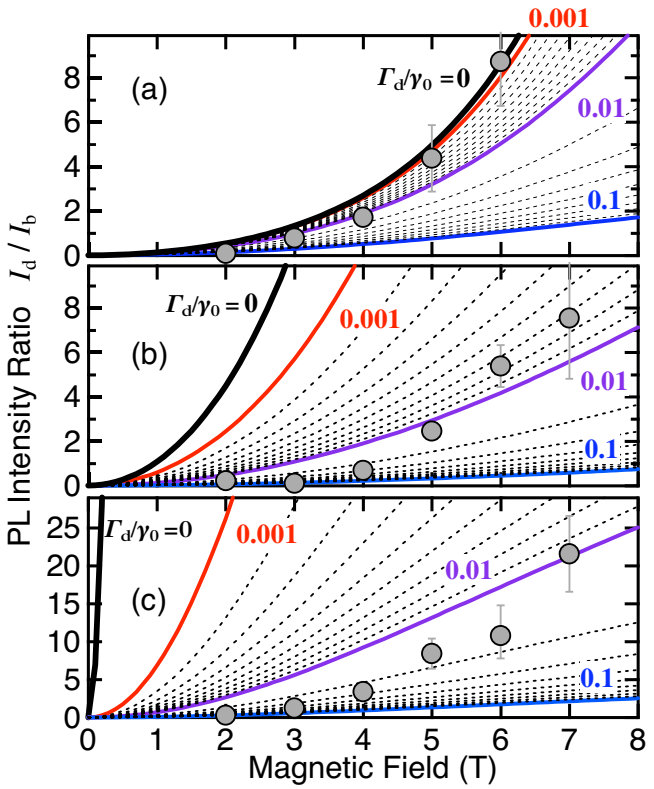

FIG. 4. (Color online) The PL intensity ratio I_d/I_b as a function of magnetic field for different nanotubes; (a) (11,3) at 9 K, (b) (7,6) at 9 K, and (7,5) at 7 K. Solid circles show experimental results and the lines indicate the calculated results for each Γ_d/γ_0.

The discrepancy of I_d/I_b in Figs. 4(a)–4(c) between the data and the solid black line (Boltzmann distribution) significantly depends on the tube diameter. The tube-diameter dependence between Figs. 4(a)–4(c) arises from the splitting energy Δ_{bd} and the AB flux. For a small-diameter tube, I_d/I_b in the black solid line (Boltzmann distribution) diverges very rapidly as a function of B, because of the large Δ_{bd}.[17] In addition, because the AB flux is proportional to the square of the diameter, exciton distribution in a larger-diameter tube is more sensitive to the magnetic field and thus comes close

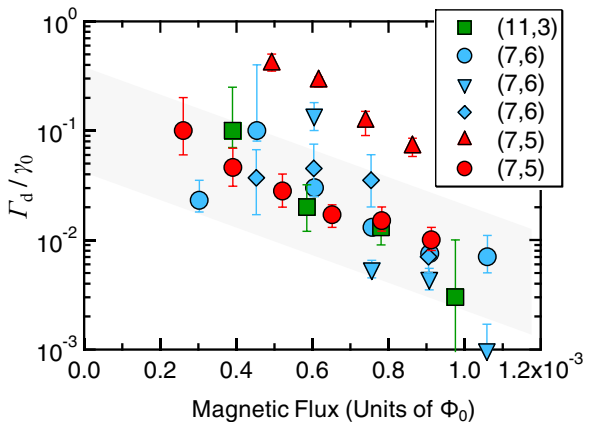

FIG. 5. (Color online) The transition rate ratio Γ_d/γ_0 for each single nanotube as a function of the AB flux by unit of the magnetic quantum $\phi_0 = ch/e$. The broad shaded line shows a guide for eyes.

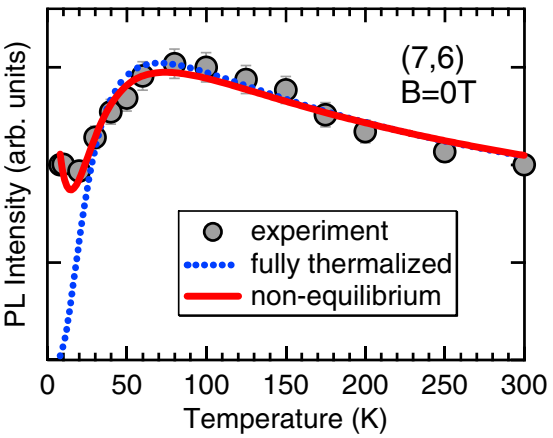

FIG. 6. (Color online) Temperature dependence of ensemble-averaged PL intensity for (7,6) carbon nanotubes dispersed in PFO (circles). The dotted line shows the calculated result using Eq. (4) with Δ_{bd}=4.5 meV assuming the Boltzmann exciton distribution. The solid line shows the calculated result using Eq. (5) with Δ_{bd} =5.6 meV and Γ_d/γ_0=0.08 assuming the non-Boltzmann exciton distribution.

more rapidly to equilibrium than a smaller-diameter tube. On the other hand, we found the universal behavior of Γ_d/γ_0 in this tube-diameter range by plotting as a function of the AB flux in Fig. 5. Figure 5 shows that exciton dynamics is not so strongly dependent on the tube diameter, and that Γ_d/γ_0 is an essential parameter for the optical properties of carbon nanotubes.

Moreover, extrapolating the experimental data, we estimate Γ_d/γ_0 at 0 T as $\sim 10^{-1}$ at low temperatures. It means that the phonon-induced exciton scattering time between the bright and dark exciton states cannot be neglected against the dark exciton lifetime and that PL dynamics in carbon nanotubes is under the influence of the non-Boltzmann exciton distribution between the bright and dark states.

C. Temperature dependence of the PL intensity

Here we investigate the temperature dependence of the PL intensity of carbon nanotubes without magnetic fields to examine the non-Boltzmann exciton distribution. Figure 6 shows the temperature dependence of ensemble-averaged PL intensity (normalized at room temperature) for (7,6) carbon nanotubes dispersed in PFO (circles). It is well known that the PL intensity has a maximum at an intermediate temperature due to the existence of the underlying dark exciton state.[12] If excitons are fully thermalized between the bright and dark states, the PL intensity of carbon nanotubes can be expressed as[12]

$$I_b \propto \frac{1}{\sqrt{T}} \frac{\exp(-\Delta_{bd}/k_B T)}{1+\exp(-\Delta_{bd}/k_B T)}, \tag{4}$$

where $T^{-1/2}$ comes from the radiative recombination rate of one-dimensional excitons[34,35] and we assumed that Γ_{NR} is temperature independent.[12] The calculated I_b from Eq. (4) with $\Delta_{bd} \sim 5$ meV is shown as a blue dotted line in Fig. 6, and it drops down to zero with $T \to 0$ because of the concen-

tration of exciton population into the dark state. In contrast, the experimentally obtained PL intensity does not become zero with $T \rightarrow 0$.[12,13]

Previously the discrepancy between the experimental data and the calculation using Eq. (4) at low temperatures has been explained by the dark exciton brightening induced by symmetry breaking due to some defects or impurities.[12,13] That is, PL at low temperatures is mostly dominated by the dark excitons and therefore strongly depends on the sample preparation. However, clear evidence for the dark exciton brightening without magnetic fields has not been reported by the magneto-PL spectroscopy for single carbon nanotubes.[17,18] In our model assuming the nonequilibrium distribution, on the other hand, the Boltzmann factors in Eq. (4) are replaced by

$$\frac{N_b}{N_d} = \exp(-\Delta_{bd}/k_B T) + \frac{\Gamma_d}{\gamma_0}[1 - \exp(-\Delta_{bd}/k_B T)], \quad (5)$$

which shows the nonzero exciton population in the bright state with $T \rightarrow 0$. Using this model, we can well reproduce the temperature dependence of the PL intensity as shown in Fig. 6 (red solid line) without the term of the dark exciton brightening. The value of Γ_d/γ_0 fitted here is about 0.08 at low temperatures[36] and consistent with the results in Fig. 5. That is, both results of the magneto-PL spectroscopy shown in Sec. III B and the temperature dependence of PL intensity can be explained by the same model of non-Boltzmann exciton distribution assuming the value $\Gamma_d/\gamma_0 \sim 10^{-1}$ at low temperatures. Our results also propose that the experimentally obtained nonzero PL intensity at low temperatures comes from the bright excitons due to the slow exciton scattering between the bright and dark states.

IV. CONCLUSION

In summary, we reported temperature-dependent magneto-PL spectra in single carbon nanotubes suspended over fabricated grooves. Direct observation of the dark exciton PL peak by single nanotube spectroscopy revealed an anomalous exciton distribution. We found that the phonon-induced exciton scattering rate from the bright to the dark states is only one order of magnitude larger than the dark exciton recombination rate at low temperatures and that excitons are not fully thermalized between the bright and dark states. Symmetry breaking induced by the AB flux enhances the phonon-induced exciton scattering between the two states. Moreover, we concluded that the nonzero PL intensity at very low temperatures comes from the bright excitons rather than the dark excitons.

ACKNOWLEDGMENTS

The authors thank H. Ajiki for helpful discussions and S. Kasai and T. Ono for technical support in fabricating the grooved Si substrates. R. Matsunaga and Y. Miyauchi were financially supported by JSPS (Grants No. 21-1890 and No. 20-3712). This study was supported by a Grant-in-Aid for Scientific Research from JSPS (Grant No. 20340075) and from MEXT of Japan (Grants No. 20048004 and No. 20104006), and the Kyoto University G-COE program from MEXT of Japan.

*matsuda@scl.kyoto-u.ac.jp
†kanemitu@scl.kyoto-u.ac.jp

[1] F. Wang, G. Dukovic, L. E. Brus, and T. F. Heinz, Science **308**, 838 (2005).
[2] T. Ando, J. Phys. Soc. Jpn. **66**, 1066 (1997).
[3] T. Ogawa and T. Takagahara, Phys. Rev. B **43**, 14325 (1991).
[4] H. Zhao and S. Mazumdar, Phys. Rev. Lett. **93**, 157402 (2004).
[5] V. Perebeinos, J. Tersoff, and Ph. Avouris, Phys. Rev. Lett. **92**, 257402 (2004).
[6] V. Perebeinos, J. Tersoff, and Ph. Avouris, Nano Lett. **5**, 2495 (2005).
[7] C. D. Spataru, S. Ismail-Beigi, R. B. Capaz, and S. G. Louie, Phys. Rev. Lett. **95**, 247402 (2005).
[8] T. Ando, J. Phys. Soc. Jpn. **75**, 024707 (2006).
[9] H. Ajiki and T. Ando, J. Phys. Soc. Jpn. **62**, 1255 (1993).
[10] S. Zaric, G. N. Ostojic, J. Kono, J. Shaver, V. C. Moore, M. S. Strano, R. H. Hauge, R. E. Smalley, and X. Wei, Science **304**, 1129 (2004).
[11] S. Zaric, G. N. Ostojic, J. Shaver, J. Kono, O. Portugall, P. H. Frings, G. L. J. A. Rikken, M. Furis, S. A. Crooker, X. Wei, V. C. Moore, R. H. Hauge, and R. E. Smalley, Phys. Rev. Lett. **96**, 016406 (2006).
[12] I. B. Mortimer and R. J. Nicholas, Phys. Rev. Lett. **98**, 027404 (2007).
[13] J. Shaver, J. Kono, O. Portugall, V. Krstic, G. L. J. A. Rikken, Y. Miyauchi, S. Maruyama, and V. Perebeinos, Nano Lett. **7**, 1851 (2007).
[14] I. B. Mortimer, L.-J. Li, R. A. Taylor, G. L. J. A. Rikken, O. Portugall, and R. J. Nicholas, Phys. Rev. B **76**, 085404 (2007).
[15] J. Shaver, S. A. Crooker, J. A. Fagan, E. K. Hobbie, N. Ubrig, O. Portugall, V. Perebeinos, Ph. Avouris, and J. Kono, Phys. Rev. B **78**, 081402(R) (2008).
[16] A. Nish, R. J. Nicholas, C. Faugeras, Z. Bao, and M. Potemski, Phys. Rev. B **78**, 245413 (2008).
[17] R. Matsunaga, K. Matsuda, and Y. Kanemitsu, Phys. Rev. Lett. **101**, 147404 (2008).
[18] A. Srivastava, H. Htoon, V. I. Klimov, and J. Kono, Phys. Rev. Lett. **101**, 087402 (2008).
[19] M. Pope and C. E. Swenberg, *Electronic Processes in Organic Crystals and Polymers* (Oxford University Press, New York, 1999).
[20] P. D. J. Calcott, K. J. Nash, L. T. Canham, M. J. Kane, and D. Brumhead, J. Phys.: Condens. Matter **5**, L91 (1993).
[21] M. Nirmal, D. J. Norris, M. Kuno, M. G. Bawendi, Al. L. Efros, and M. Rosen, Phys. Rev. Lett. **75**, 3728 (1995).
[22] F. Wang, G. Dukovic, L. E. Brus, and T. F. Heinz, Phys. Rev. Lett. **92**, 177401 (2004).
[23] A. Hagen, M. Steiner, M. B. Raschke, C. Lienau, T. Hertel, H.

Qian, A. J. Meixner, and A. Hartschuh, Phys. Rev. Lett. **95**, 197401 (2005).
[24] H. Hirori, K. Matsuda, Y. Miyauchi, S. Maruyama, and Y. Kanemitsu, Phys. Rev. Lett. **97**, 257401 (2006).
[25] G. Scholes, S. Tretiak, T. McDonald, W. Metzger, C. Engtrakul, G. Rumbles, and M. Heben, J. Phys. Chem. C **111**, 11139 (2007).
[26] S. Berger, C. Voisin, G. Cassabois, C. Delalande, P. Roussignol, and X. Marie, Nano Lett. **7**, 398 (2007).
[27] S. Berciaud, L. Cognet, and B. Lounis, Phys. Rev. Lett. **101**, 077402 (2008).
[28] S. Maruyama, R. Kojima, Y. Miyauchi, S. Chiashi, and M. Kohno, Chem. Phys. Lett. **360**, 229 (2002).
[29] J. Lefebvre, Y. Homma, and P. Finnie, Phys. Rev. Lett. **90**, 217401 (2003).
[30] T. Inoue, K. Matsuda, Y. Murakami, S. Maruyama, and Y. Kanemitsu, Phys. Rev. B **73**, 233401 (2006).
[31] K. Matsuda, T. Inoue, Y. Murakami, S. Maruyama, and Y. Kanemitsu, Phys. Rev. B **77**, 033406 (2008).
[32] K. Matsuda, T. Inoue, Y. Murakami, S. Maruyama, and Y. Kanemitsu, Phys. Rev. B **77**, 193405 (2008).
[33] A. Nish, J.-Y. Hwang, J. Doig, and R. J. Nicholas, Nat. Nanotechnol. **2**, 640 (2007).
[34] D. S. Citrin, Phys. Rev. Lett. **69**, 3393 (1992).
[35] H. Akiyama, S. Koshiba, T. Someya, K. Wada, H. Noge, Y. Nakamura, T. Inoshita, A. Shimizu, and H. Sakaki, Phys. Rev. Lett. **72**, 924 (1994).
[36] We used a temperature-independent value of $\Gamma_d/\gamma_0=0.08$ for simplification. In fact, Γ_d/γ_0 should increase with temperature as shown in Fig. 3(b). But at higher temperatures above 100 K, the value of Γ_d/γ_0 has an insignificant effect on the calculated curve in Fig. 6 due to the increase in $\exp(-\Delta_{bd}/k_BT)$ term in Eq. (5).